Nanocrystals as an effective strategy to improve Pomalidomide bioavailability in rodent

Maria Cristina Cardia[1], Maria Francesca Palmas[2], Luca Casula[1], Augusta Pisanu[3], Salvatore Marceddu[4], Donatella Valenti[1], Chiara Sinico[1], Elena Pini[5], Michael T. Scerba[6], David Tweedie[6], Nigel H. Greig[6], Anna Rosa Carta[2*], Francesco Lai[1*]

[1]Department of Life and Environmental Sciences, Unit of Drug Sciences, University of Cagliari, Cagliari, Italy

[2]Department of Biomedical Sciences, University of Cagliari, Cagliari, Italy,

[3]National Research Council, Institute of Neuroscience, Cagliari, Italy

[4]Institute of Sciences of Food Production (ISPA-CNR), Baldinca (Sassari), Italy

[5] Department of Pharmaceutical Sciences, Università degli Studi di Milano, Italy

[6]Drug Design & Development Section, Translational Gerontology Branch, Intramural Research Program, National Institute on Aging, National Institutes of Health, Baltimore, MD, United States

Abstract

Pomalidomide (POM) is an FDA-approved immunomodulatory imide drug (IMiDs) an it is effectively used in the treatment of multiple myeloma. IMiDs are analogs of the drug thalidomide and they have been repurposed for the treatment of several diseases such as psoriatic arthritis and Kaposi Sarcoma. In recent years, IMiDs have been also evaluated as a new treatment for neurological disorders with an inflammatory and neuroinflammatory component. POM draws particular interest for its potent anti-TNF-α activity at significantly lower concentrations than the parent compound thalidomide. However, POM's low water solubility underpins its low gastrointestinal permeability resulting in irregular and poor absorption. The purpose of this work was to prepare a POM nanocrystal-based formulation that could efficiently improve POM's plasma and brain concentration after intraperitoneal injection. POM nanocrystals prepared as a nanosuspension by the media milling method showed a mean diameter of 219 nm and a polydispersity index of 0.21. POM's nanocrystal solubility value (22.97 µg/mL) in phosphate buffer was about 1.58 folds higher than the POM raw powder. Finally, in vivo studies conducted in adult Male Sprague-Dawley rats indicated that POM nanocrystal ensured higher and longer-lasting drug levels in plasma and brain when compared with POM coarse suspension.

Keywords: Pomalidomide; nanocrystals; neurological disorders; nanosuspensions; brain

*Correspondence: frlai@unica.it, tel.: +39-070-6758514; acarta@unica.it , te. +39-070/6758662

1. Introduction

Immunomodulatory imide drugs (IMiDs) are analogs of the drug thalidomide, and have been repurposed for the treatment of several diseases such as multiple myeloma, psoriatic arthritis and Kaposi Sarcoma (Bristol Myers Squibb, 2020). In recent years, IMiDs have been evaluated as a new treatment strategy neurological disorders with an inflammatory and neuroinflammatory component, based on the pleiotropic action of this drug class that include potent anti-inflammatory effects consequent to their ability to inhibit the production of proinflammatory cytokines. Chronic neuroinflammation is a feature shared across neurological disorders, being a pivotal mechanism of neurodegeneration in Parkinson's disease (PD) and in Alzheimer disease (AD), but also heavily involved in the pathophysiology of psychiatric disorders (Beurel et al., 2020; Jung et al., 2021). Pathological glial cell activation, involving both microglia and astroglia, is sustained by inflammatory cytokines overproduced by the microglia itself, creating and subsequently driving a powerful self-destructive cycle that lead to neuronal dysfunction or neurotoxicity across neurodegenerative diseases (Kuter et al., 2020). Among IMiDs, Pomalidomide (POM) is a third generation FDA-approved and clinically available drug (*Pomalyst*) widely used and effective in the treatment of multiple myeloma (Siegel et al., 2020). POM draws particular interest for its potent anti-TNF-α activity at significantly lower concentrations than the parent compound thalidomide (Mahony et al., 2013), and is associated with less adverse effects in relation to teratogenic, anti-angiogenic and neurotoxic activity in animal models (Mahony et al., 2013; Vargesson et al., 2013). The inhibition of TNF-α production occurs via posttranslational mechanisms, leading to the downregulation of the inflammatory cascade (Chanan-Khan et al., 2013; Moreira, 1993; Sampaio et al., 1991; Terpos et al., 2013; Tweedie et al., 2011). POM was reported to suppress inflammation-induced neuronal injury in cells and animal models of neurological diseases and cellular stress (Wang et al. 2016; Tsai et al. 2018, 2019; Lin et al., 2020). Moreover, a recent study demonstrated the neuroprotective efficacy of POM in the drosophila LRRK2 genetic model of PD (Casu et al., 2020; Dues and Moore, 2020), and the disease-modifying properties of POM have been observed in the α-synuclein-based neuropathological model of PD in rat (Palmas et al., in preparation) as well as rats challenged with traumatic brain injury (Lin et al., 2020).

In relation to the use of IMiDs in neurological disorders, most molecules of this class show high CNS MPO (multiparameter optimization) scores, which provides a quantitative prediction of drug blood-brain barrier (BBB) permeability/uptake (Jung et al., 2019; Wager et al., 2010). Specifically, POM has a favorable brain uptake in rats and mice, achieving a brain/plasma concentration ratio in the range of 0.39 to 0.71 (Jiang et al. 2014; European Medicines Agency 2019; Tsai et al. 2019), which positions this drug as a high choice compound in the IMiD drug class for repositioning in neurological disorders.

On the other hand, the favorable CNS MPO score and brain partitioning contrasts with POM's low water solubility and lipophilicity, which are independent of pH, and underpin its low gastrointestinal permeability (putting it in class IV of the BCS (Biopharmaceutics Classification System) for drug administration) (Amidon et al., 1995), resulting in irregular and poor absorption. Indeed, an assessment of POM's oral bioavailability in rats and monkeys at a dose of 100 mg/kg provided a low value of 13% to 15%, which dramatically contrasts with a high bioavailability of approximately 100% when administered at a 2 mg/kg dose in monkeys (European Medicines Agency 2019), clearly signifying that absorption is solubility limited. For this drug class an improvement in dissolution rate and solubility is hence a key parameter to ameliorate drug gastrointestinal adsorption inadequacies (Ghadi and Dand, 2017). Among all the formulation strategies developed in attempts to improve bioavailability of BCS class IV drugs, the crystal nanosizing process represents one of the most efficient approaches (Lai et al., 2018; Wang et al., 2021). The nanocrystals obtained with this process have been defined as crystals of pure drug with a mean diameter below 1 micron (Müller et al., 2001). They are prepared as a dispersion in water and/or water-miscible solvent and stabilized using ionic, non-ionic surfactant or polymer (Müller and Peters, 1998). The large surface area of nanocrystals enhances both drug dissolution and drug saturation solubility and, thereby, promotes adsorption and bioavailability (Corrias et al., 2017; Gao et al., 2013; Manca et al., 2020).

The purpose of this work was to prepare a POM nanocrystal-based formulation (POM-NS) that could efficiently improve POM's plasma and brain concentration after intraperitoneal injection. Intraperitoneal drug administration is amongst the common routes used for toxicological studies in rodent. Here, we decided to use the intraperitoneal route in order to mimic the oral administration as regard to portal adsorption and first-pass liver metabolism, yet assuring a homogeneous interindividual bioavailability as compared to oral intake (Hoffmann et al., 2013; Lukas et al., 1971). POM-NS was prepared as a nanosuspension by a top down – media milling method using Polysorbate 80 as stabilizer. The nanocrystal mean size, size distribution and zeta potential were determined by dynamic light scattering on the day of preparation and during a stability test period of two months. Solubility and dissolution studies were carried out at 37 °C in phosphate buffer solution (PBS) with a pH of 7.4 to simulate the peritoneal conditions. The morphology of the formulations was assayed by Scanning Electron Microscopy (SEM). Finally, *in vivo* studies were conducted in adult Male Sprague-Dawley rats to evaluate the POM plasma and brain concentrations after intraperitoneal administration of POM-NS using a suspension of the raw drug (POM-CMCS) as a reference formulation.

2. Materials and Methods

Materials

Polysorbate 80 (Tween 80) was purchased from Galeno (Comeana, Italy). Acetonitrile, DMSO and all the other products were supplied by Sigma Aldrich (Milan, Italy).

Animals

Male Sprague-Dawley (Envigo, Italy) rats (275-300 g), housed in groups of four, were acclimatised at 21 ± 1°C; 60% on a 12 h light/dark cycle (lights on at 7:00 a.m.). All experimental procedures complied with the ARRIVE guidelines and were in accordance with the guidelines and protocols approved by the European Community (2010/63UE L 276 20/10/2010). Experimental protocols were approved by the Ministry of Health, Autorization n° 766/2020-PR (D.lgs. 26/2014).

Synthesis of POM

Pomalidomide (4-amino-2-(2,6-dioxopiperidin-3-yl) isoindole-1,3-dione) was generated via a two-step synthetic scheme. Initially, 3-aminopiperidine-2,6-dione was condensed with 3-nitrophthalic anhydride in refluxing acetic acid. Sequential precipitation over ice water (0°C) provided the resultant nitro-thalidomide as a grey-purple solid. Subsequent hydrogenation over a palladium catalyst provided POM. Finally, POM was recrystallized from DMSO and water. The resulting isolated POM crystals were thereafter washed in water and then further dried under vacuum to give a yellow powder. The compound was structurally characterized by ^{1}H and ^{13}C NMR (spectra reported in Supporting Material). LC/MS and HRMS were performed to further confirm the chromatographic signatures and molecular formula. Elemental analysis confirmed a minimum 95% purity.

Preparation and Characterization of POM Nanosuspensions (POM-NS)

POM nanosuspension (POM-NS) was prepared using the Wet media milling technique. The bulk drug (1.5%) was dispersed in an aqueous solution of Tween 80 (0.75%) and vortexed for 7 min. The obtained suspension was then placed in 5 eppendorf microtubes containing 0.4 g of 0.1–0.2 mm yttrium-stabilized zirconia-silica beads (Silibeads® Typ ZY Sigmund Lindner, Germany). The microtubes were oscillated at 3000 rpm for 45 min using a beads-milling cell disruptor equipment (Disruptor Genie®, Scientific Industries, USA). The obtained nanosuspension was collected from each microtube and sieved to separate the zirconia-silica beads. The nanosuspension was then characterised by dynamic light scattering (DLS) using a Zetasizer nano (Malvern Instruments, Worcestershire, UK) to allow determination of the size (mean diameter) and polydispersity index (PDI), a measure of the size distribution width. Zeta potential was measured

using the Zetasizer nano by employing the M3-PALS (Phase Analysis Light Scattering) technique. Immediately prior to analysis, POM nanosuspension was diluted with bi-distilled water (1:100). A long-term stability study of POM-NS stored at room temperature was performed by monitoring mean diameter, PDI and Zeta potential for 60 days.

Solid state characterization

ATR-FT-IR spectra were acquired with a Perkin Elmer Spectrum One FT-IR (Perkin Elmer, Waltham, MA, USA), equipped with a Perkin Elmer Universal ATR sampling accessory consisting of a diamond crystal. Analyses were performed in a spectral region between 4000 and 650 cm^{-1} and analysed by transmittance technique with 28 scansions and 4 cm^{-1} resolution.

Differential Scanning Calorimetry analyses were performed to characterize the thermal behavior of POM and corresponding nanosuspension using a Perkin Elmer DSC 6 Waltham, MA, USA. All experiments were conducted at a heating rate of 10 °C/min up to 350 °C in a nitrogen atmosphere purging nitrogen at a flow rate of 20 mL/min. Samples (2-3 mg) were hermetically sealed in an aluminum pan and a control empty pan subjected to the same heating conditions was used as reference.

The XRPD analyses were performed with a Rigaku MiniFlex diffractometer by using a CuKα radiation detector (λ = 1.54056 Å) as source of X-rays. The voltage and current were of 30 kV and 15 mA, respectively. Measurements were undertaken at scan angular speed of 2 °C/min, and a scan step time of 2.00 s in the range from 3° to 60 °C. The diffractograms are expressed as peak intensity versus 2θ.

Preparation of POM coarse suspension (POM-CMCS)

Drug coarse suspension (1.5%) was obtained by dispersing bulk POM in a 1% carboxy methyl cellulose (CMC) solution. The dispersion was homogenised by using an Ultra Turrax T25 basic (IKA, Werke) for 5 min at 6500 rpm.

Scanning Electron Microscopy

The morphology of nanocrystals and bulk POM was evaluated using Scanning Electron Microscopy (SEM). Bulk POM was mounted on an aluminium stub with carbon adhesive discs and coated with gold in an Agar Automatic Sputter Coater B7341, and examined with an environmental scanning electron microscopy (Zeiss EVO LS 10, Oberkochen, Germany) operating at 20 Kv, in hight vacuum mode with a secondary electron detector (SEI). For the nanocrystals SEM morphologic investigation, a drop of POM nanosuspension was placed on a slide and air dried, coated with gold in an Agar Automatic Sputter Coater B7341 and examined with the same instrument at 20 Kv, in hight vacuum mode with SEI.

Solubility Studies

POM solubility was measured at 37 °C in phosphate buffer solution (PBS) with a pH of 7.4 to simulate the peritoneal conditions. An excess of POM raw powder, POM coarse suspension or POM nanosuspension (n = 3) were kept under constant stirring for 72 h at 37°C. Samples were withdrawn and centrifuged at 15,000 rpm for 60 min; the supernatant was centrifuged again at 15,000 rpm for 20 min. Then, a known amount of the clear supernatant was withdrawn and diluted with CH_3CN:DMSO (50:50) for HPLC analysis.

Dissolution Studies

POM dissolution experiments were carried out at 37 °C in phosphate buffer solution (PBS) with a pH of 7.4. 1.5 mg of POM as bulk powder or POM-NS or a coarse crystals suspension were added to 100 mL of PBS at 37 °C. The release cells were constantly stirred using a magnetic stirrer and kept at 37 °C throughout the study. The amount of POM and the PBS volume were calculated in order to avoid the saturation of the release medium. At regular time intervals, a 2 mL volume was withdrawn and immediately centrifuged at 15000 rpm for 20 minutes in order to separate the undissolved POM. The supernatant was then analyzed by HPLC for POM quantification.

Pomalidomide HPLC Quantification

POM content was determined at an excitation wavelength of 235 nm and an emission wavelength of 472 nm using a chromatograph Alliance 2690 (Waters, Italy) equipped with a multi λ fluorescence detector and computer integrating software (Empower 3). The column was a X Terra RP18 (3.5 µm, 4.6 mm × 100 mm, Waters), and the mobile phase was a mixture of water: ACN: Acetic acid =20: 84.5: 0.5, eluted at a flow rate of 0.7 mL/min, RT= 1.65 min. A standard calibration curve was generated by using standard solutions. Calibration graphs were plotted according to the linear regression analysis, which gave a correlation coefficient value (R^2) of 0.999. The limit of quantification (LOQ) of POM was 1pg, the limit of detection (LOD) was 0.01pg.

Pharmacological treatments

Rats were randomly divided into 10 groups (3 rats per group) and were i.p. injected with a single dose of POM-NS (20 mg/kg) or POM-CMCS (20 mg/kg). After treatment, the animals were deeply anesthetized and sacrificed by decapitation after 30 min, 2, 6, 24 and 48 h to collect blood and brain samples. These were immediately frozen and stored at -80°C prior to analyses.

Preparation of blood samples for Pomalidomide HPLC analyses

Heparinized plasma samples (600µL) were treated with a mixture of ACN/DMSO 50% (600µL). The mixture was vortexed for 2 min and then centrifuged for 25 min at 15000 rpm at 4°C. The supernatant was separated from the pellet and placed in tubes for HPLC analysis.

Preparation of brain samples for Pomalidomide HPLC analyses

The brain of each rat was thawed, carefully weighed and shredded in a mortar with the help of a pestle to homogenize the samples. Homogenates were treated with a mixture of ACN/ DMSO 50% (5 mL) and collected in a tube. Samples were vortexed for 30 min, using an ice bath to avoid overheating, and then divided into five Eppendorf tubes. Samples were then centrifugated for 25 min at 15000 rpm (4°C) and the supernatant was recovered in tubes for HPLC analysis.

Pharmacokinetic Analysis

Pharmacokinetic parameters (PK) were determined using the PK-Solver software (in the non-compartmental analysis mode) and the POM mean plasma concentration (n = 3 determinations at each time point) after a single i.p. administration of POM-NS or POM-CMCS. The elimination half-life ($T_{1/2}$) was determined as 0.693/ elimination rate constant, whereas the $AUC_{0-\infty}$ (the total area under the drug plasma concentration–time curve) was calculated using the trapezoidal method.

Statistical Analysis of Data

Results are expressed as the mean ± standard deviation, and significance was tested at the 0.01 or 0.05 level of probability (p). For POM plasma and brain levels, analysis of variance (one way-ANOVA) followed by post-hoc Bonferroni correction were used to substantiate statistical differences between groups using XLSTAT for Excel.

3. Results

Characterization of POM Nanosuspensions

In this work, aiming at improving the bioavailability of POM after intraperitoneal injection in rats, POM nanosuspension (POM-NS) was prepared using the wet media milling technique and was stabilized with the non-ionic surfactant Tween 80 (0.75%, Table 1). Freshly prepared POM-NS shows a mean diameter of 219 nm and a polydispersity index (PDI) of 0.21, demonstrating a relatively narrow size distribution (Table 1). The strongly negative zeta potential value (-43 mV) should ensure POM-NS stability against aggregation phenomena across time.

A long-term POM-NS stability study was performed for 60 days, monitoring the variations in size, PDI, and Zeta Potential of nanocrystals stored at 25 °C (Figure 1). As shown in Figure 1, no appreciable variation in size and PDI was observed during the monitoring time. Only at day 14 and 21 a slightly increase of the nanocrystals mean diameter and PDI was evident. Furthermore, during 60 days of storage, the POM-NS Zeta Potential remained strongly negative (-45/-50mV).

Table 1. Composition and characterization of POM-NS at the day of preparation.

POM-NS composition		**Characterization**		
Component	% (w/w)	Mean diameter (nm)	PDI	Zeta Potential (mV)
Pomalidomide	1.5			
Tween 80	0.75	219±2	0.21±0.02	-43 mV±1
Water	97.75			

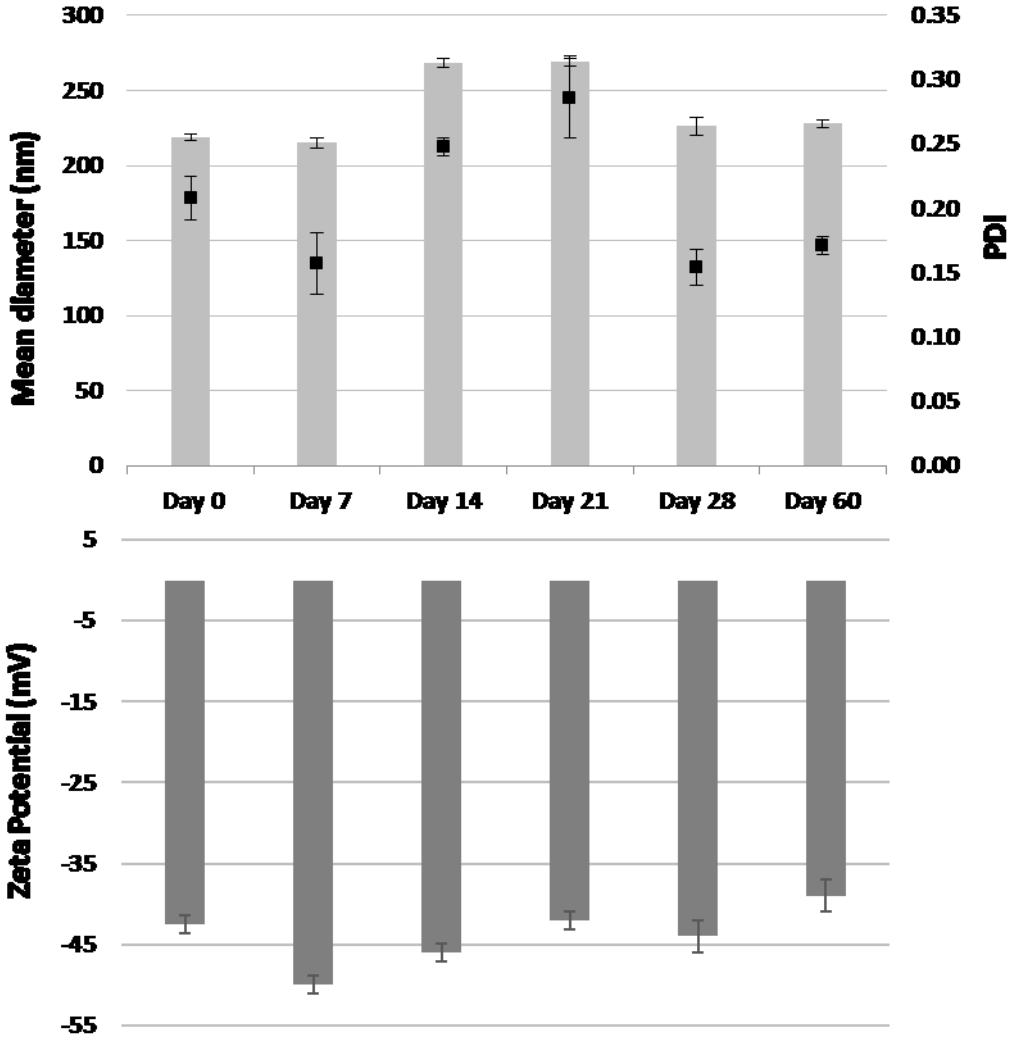

Figure 1. Mean diameter, polydispersity index (PDI) and Zeta Potential of POM-NS during 60 days of storage at 25°C. Results are expressed as means of three independent measurements ± standard deviation.

Scanning Electron Microscopy

SEM micrographs were performed to investigate both the morphology and the size of bulk POM powder and POM-NS (Figure 2 A-D). POM bulk powder appears as clusters of irregular large crystals, with heterogeneous dimensions that can exceed 5 µm. In contrast, POM-NS revealed a definite multifaceted structure, and a regular and homogeneous arrangement. Moreover, SEM analyses confirmed that the mean diameter of nanocrystals is comparable to that measured by dynamic light scattering.

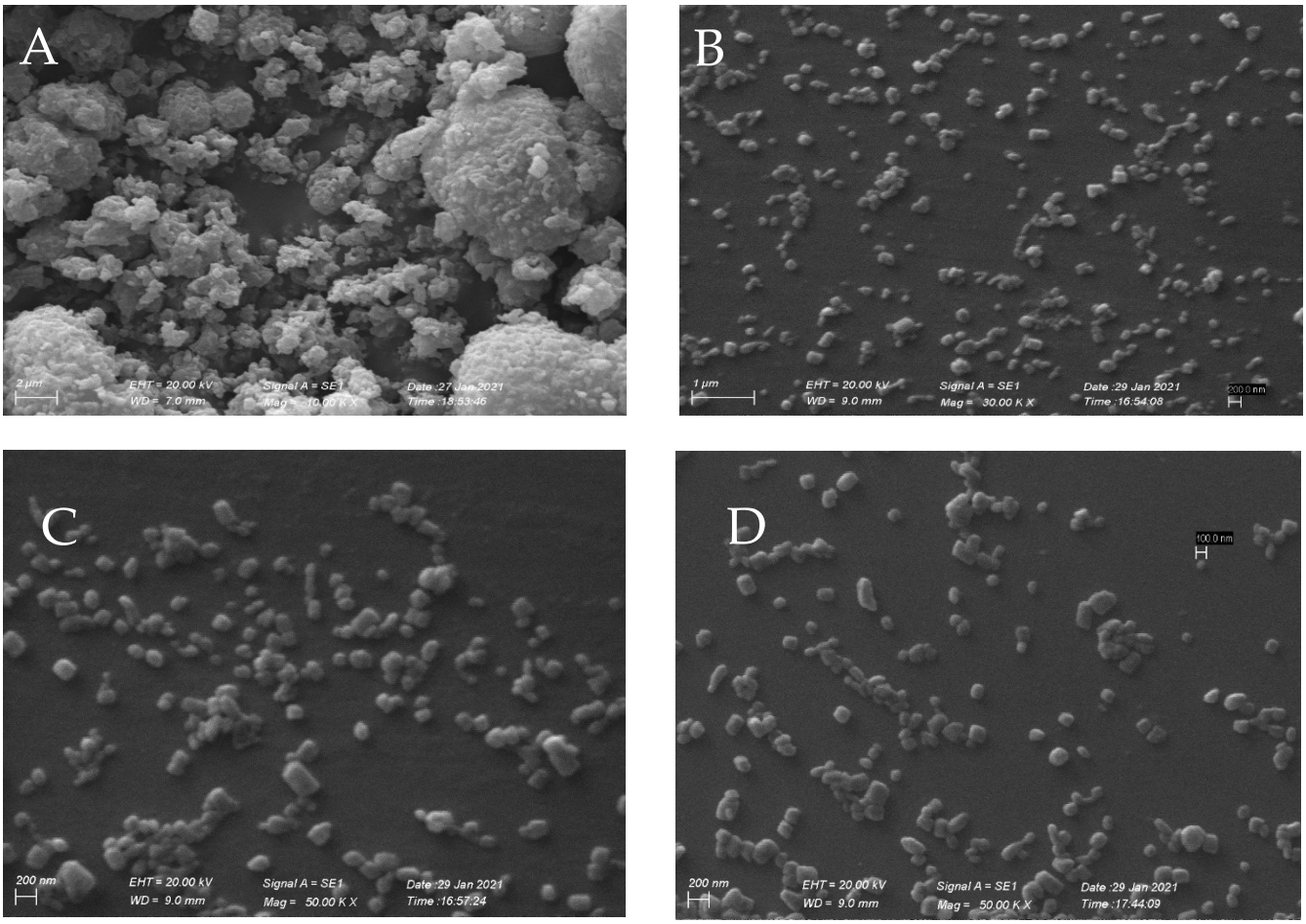

Figure 2. SEM micrographs showing the morphology and the size of bulk POM powder (A) and POM-NS (B, C and D).

DSC analyses

DSC thermograms of POM and the corresponding lyophilized nanosuspension powder, are shown in Fig.3 . The DSC trace of raw POM (Fig. 3a) showed a sharp peak at 313.98 °C which corresponds to the drug melting point with a fusion enthalpy $\Delta Hm = 147.12$ J/g. The presence of a sharp peak indicates the crystalline nature of the drug. In the nanosuspension thermogram (Fig. 3b) two endothermic peaks are shown at 116 ° and 307 °C which correspond to the tween 80 flash point (Pramod et al., 2015), and to the crystalline POM melting event, respectively. The POM endotherm is slightly shifted towards a lower temperature, possibly due to the drug's small particle size in the nanocrystalline suspension, dissolution of the drug in the stabilizer during the DSC run, or strong interaction between the drug and the stabilizer, as also suggested by the decreased enthalpy of POM in the formulation.

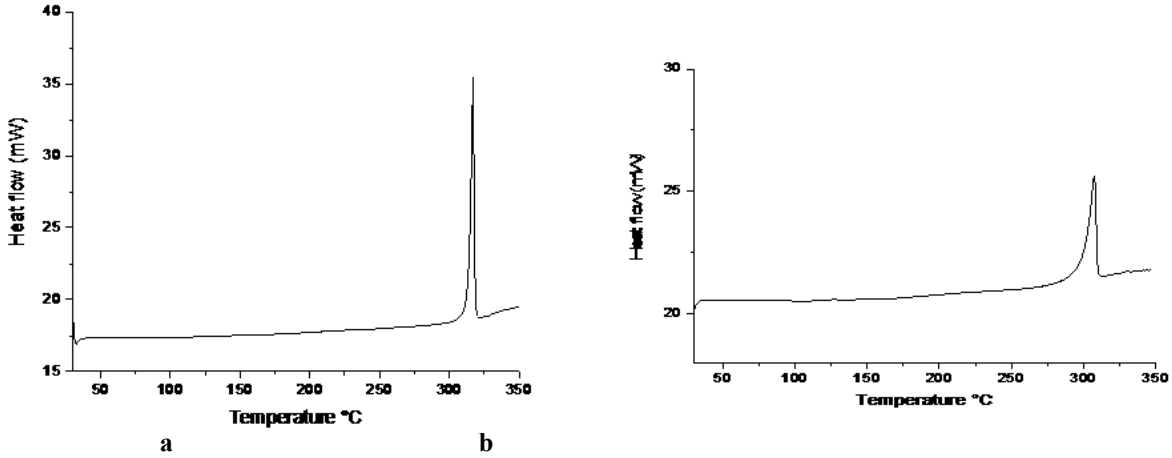

Figure 3. DSC Pomalidomide (a) and ns Pomalidomide (b)

ATR-FTIR

Figure 4 presents the ATR Infrared spectrum superimposition of POM, tween 80 and POM-NS. The superimposition revealed the lack of appearance of new peaks and the lack of disappearance of existing peaks, indicating that the drug and the stabilizer do not interact with each other.

In fact, in the lyophilized nanosuspension spectrum were identified the POM NH_2 at 3481 and 3377 cm^{-1}, the H-C= and H-C- stretchings at 3113, 2984, 2898 respectively, the C=O stretchings at 1751, 1726, 1691 and 1632, the C=C bands at 1594 and 1477, the C-N and C-O vibrations at 1408, 1358, 1320 cm^{-1}. Furthermore, some tween 80 signals at 2859 (CH_2-stretching), and around 1100 (C-O-stretching), are detectable.

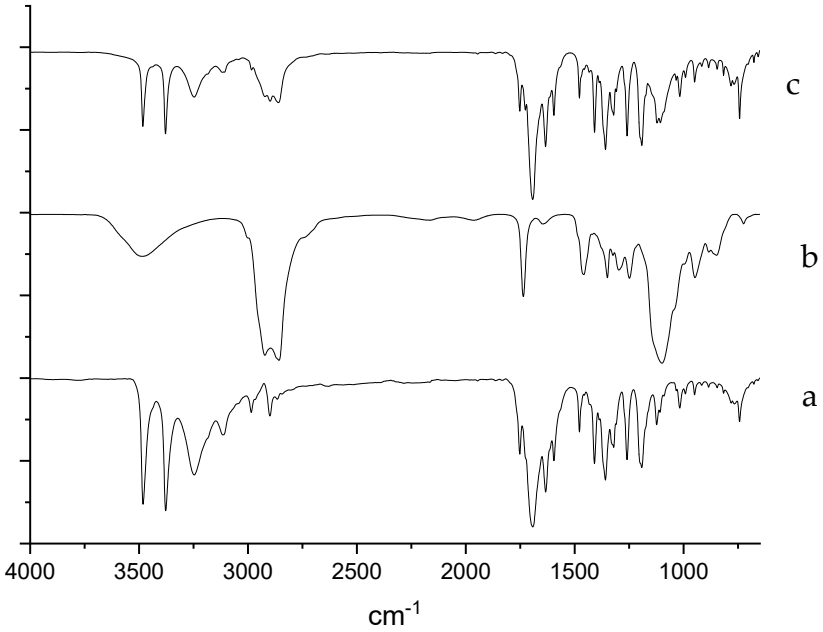

Figure 4: ATR-FTIR POM (a), Tween 80 (b) and POM-NS (c) **.**

XRPD

The XRPD spectra of bulk POM powder and POM-NS are shown in Figure A of Supporting Material. In agreement with literature data (Szabó et al., 2021) the sharp diffraction peaks of bulk POM powder at 12.3, 14.1, 16.9, 17.3, 18.3, 24.3, 24.7, 25.6, and 28.0 2ϑ indicate its crystalline nature. Also in the POM-NS diffractogram the characteristic peaks of POM are clearly evident, thus suggesting that its crystal pattern is not affected by the formulation process. However, the decreased peak intensity showed in figure, should be due to the particles size reduction to the nanometer range.

Solubility Studies

As shown in the Figure 5, the solubility of POM as a raw powder was 14.53 ± 0.41 µg/mL. Interestingly, the formulation of the coarse suspension with the same drug/surfactant ratio of the nanosuspension, did not lead to an increase of POM solubility, which resulted to be 13.02 ± 1.33 µg/mL. On the other hand, POM-NS showed a solubility value of 22.97 ± 4.03 µg/mL, which was 1.58 folds higher than the raw powder. Therefore, these results demonstrate that POM solubility is not enhanced by the action of the surfactant, but mostly by the nanosizing of the particles, in accordance with the Freundlich-Ostwald equation (Müller and Peters, 1998).

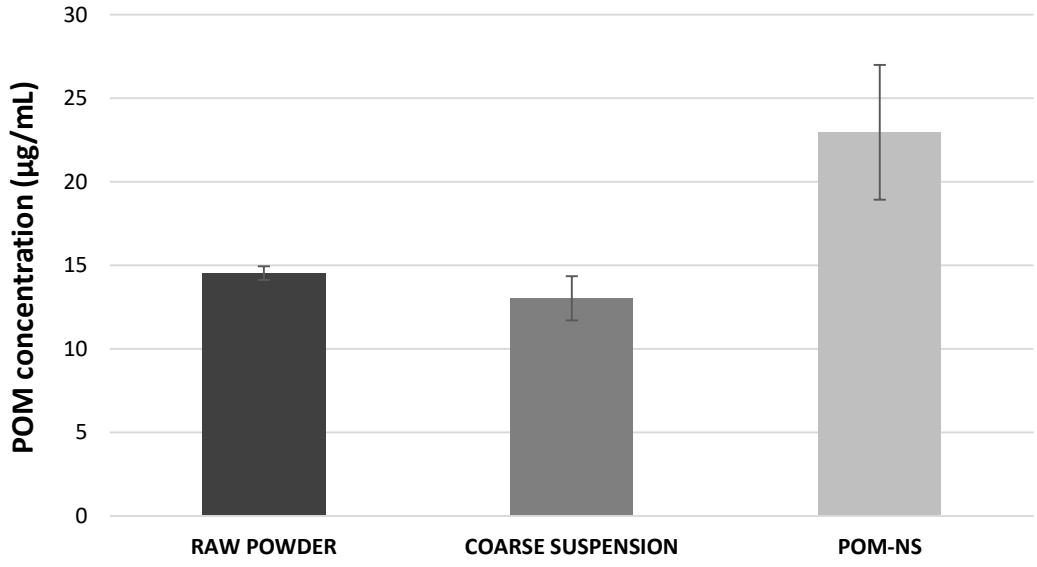

Figure 5. Solubility of raw POM, POM coarse suspension and POM nanosuspension (POM-NS) in phosphate buffer solution at 37 °C.

Dissolution Studies

POM dissolution studies were performed at 37 °C in phosphate buffer solution with a pH of 7.4 to simulate the peritoneal conditions. Results reported in Figure 6 show an immediate and rapid dissolution of POM nanocrystals (POM-NS). Indeed, 90% of POM dissolved in the release medium as early as 1 minute. After some 3 minutes 100% of POM was in solution. On the contrary, total dissolution of POM as a coarse suspension (POM-CMCS) was reached only after 6 h. The dissolution rate of the raw drug was even slower than that of POM-CMCS, as after 8 h only 38% of raw POM dissolved into the buffer solution. This slow dissolution of POM, whether as the raw drug or as a coarse suspension, is in line with the recent studies of Szabó et al. (Szabó et al. 2021), who similarly demonstrated slow dissolution into both Britton-Robinson buffer at pH 7.0 and simulated gastric fluid at pH 1.6. The substantial increase in the the solubility of POM formulated as nanosuspension and its immediate dissolution clearly indicates that nanosizing may increase the POM absorption rate and, therefore, the bioavailability after i.p. administration (Gao et al., 2013; Lai et al., 2018). To quantitatively evaluate this, studies were performed in rats.

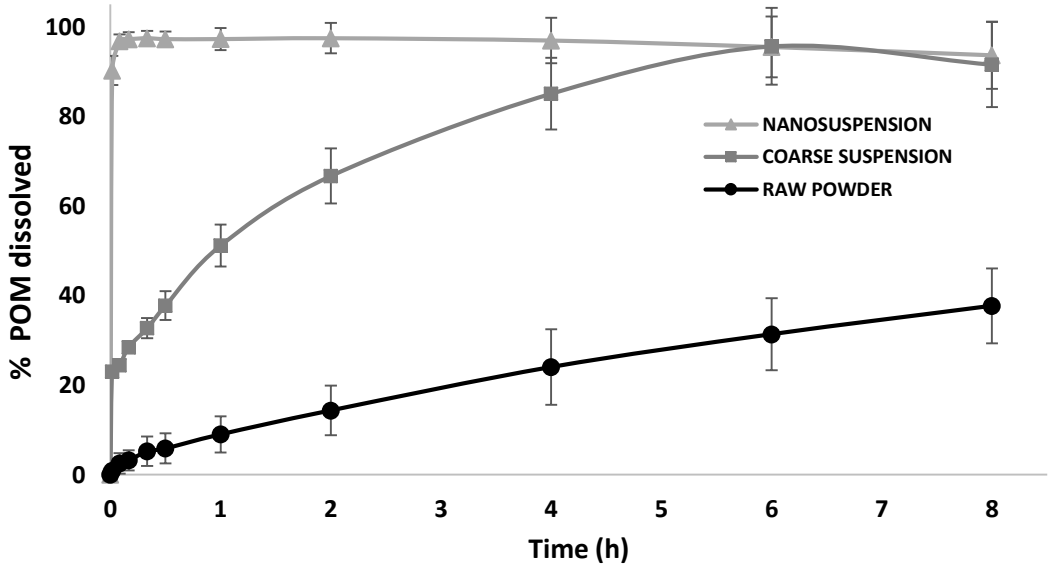

Figure 6. Dissolution profiles of raw POM, POM coarse suspension and POM nanosuspension (POM-NS).

In vivo studies

In vivo studies were conducted in adult Male Sprague-Dawley rats after a single i.p. administration of the same POM dose in different formulations (POM-NS or POM-CMCS). POM is typically taken by patients via oral formulations; however, as previously stated, we decided to use the intraperitoneal route in order to mimic the oral administration with regard to portal adsorption and first-pass liver metabolism, yet assuring a homogeneous interindividual bioavailability as compared to the oral intake (Hoffmann et al., 2013; Lukas et al., 1971). Plasma POM levels were measured at progressive time-points (0.5, 2, 6, 24 and 48 h, Figure 7A) and the PK-Solver software was used to calculate the POM pharmacokinetic parameters (Table 2). Figure 7A shows the plasma drug concentration/time curve for POM-NS or POM-CMCS. As reported in the Figure, HPLC measurement of the drug showed a peak concentration in plasma of 3.73±0.47 μg/ml at 0.5 h after intraperitoneal administration of POM-NS, that was increased to 4.09 μg/ml and moved up to 0.13 h after PK-Solver calculation. Drug levels were still elevated 2 h after administration (2.40±0.19 μg/ml) and remained detectable after 6 h, to be fully cleared from blood circulation at 24 h. Whereas POM-CMCS displayed a similar time-course, the achieved plasma concentration was always lower as compared to that measured after the POM-NS administration. Indeed, a peak plasma concentration of 2.29±0.56 μg/ml was reached 0.5 h after POM-CMCS administration based on HPLC measurement, increased to 3.06 μg/ml after 0.18 h as recalculated by the PK-Solver analysis. Moreover, analysis of the time-dependent concentration curves showed that POM was cleared more rapidly from blood when administered as a coarse suspension, as drug levels were almost undetectable after 6 h. As a consequence, the POM elimination half-life ($t_{1/2}$) obtained after the administration of POM-CMCS ($t_{1/2}$= 0.59 h) was extended to 2.45 h when POM was administered as nanosuspension (Table 2). The $AUC_{0-\infty}$ values of POM-NS (15.02 μg/ml*h) and POM-CMCS (3.24 μg/ml*h), calculated via the PK-Solver software, clearly indicate that the amount and rate of absorption of POM molecules from the peritoneal cavity were significantly higher when the nanosuspension form of the agent was administered. This difference specifically related to the nanosizing process that provided an increased solubility and dissolution rate of POM nanocrystal, as compared to the coarse crystals of the POM-CMCS.

	POM-NS	POM-CMCS
$t_{1/2}$ (h)	2.45±0.32	0.59±0.12
V_{ss} (L/kg)	4.69±1.05	5.26±1.15
CL (L/Kg/h)	1.32±0.24	6.16±1.89
T_{max} (h)	0.13±0.03	0.18±0.02
C_{max} (µg/ml)	4.09±1.15	3.06±0.86
AUC $_{0\text{-inf}}$ (µg/ml*h)	15.02±2.03	3.24±0.24

Table 2. POM PK parameters after a single i.p. administration (20 mg/kg) of POM-NS and POM-CMCS in rats. $t_{1/2}$ (Elimination half-life); T_{max} (Time to reach maximum blood concentration); C_{max} (Maximum blood concentration); V_{ss} (Apparent volume of distribution at steady state); CL (Apparent clearance); $AUC_{0-\infty}$ (the total area under the drug plasma concentration–time curve).

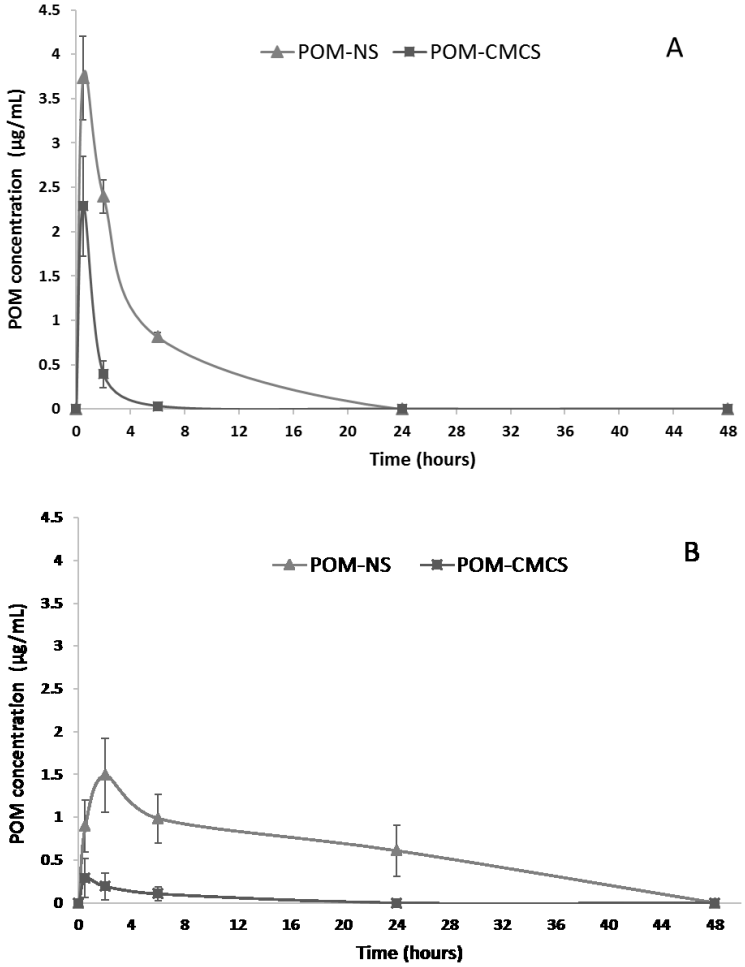

Figure 7. Plasma (A) and brain (B) POM concentration after i.p. administration of POM-NS and POM-CMC coarse suspension at increasing time points (0.5, 2, 6, 24 and 48h). Statistical analysis of the data shown in Figure 7A indicates that the concentrations of POM reached in plasma after the administration of POM-NS at the different time points (0.5, 2, 6 h) are statistically significantly different from the concentrations detected after administration of the POM-CMC (0.5 h: $p < 0.05$; other times points: $p < 0.01$). Similarly, brain concentrations measured after administration of POM-NS (Figure 7B) are significantly different from those determined after administration of CMC POM (0.5 hours: $p < 0.05$, other time points: $p < 0.01$).

Moreover, in compliance with our final aim of accomplishing a drug formulation which may improve the brain bioavailability of POM for repurposing this drug in neurological disorders, the drug brain concentration in rats treated with POM-NS and POM-CMCS was determined.

In Figure 7B the concentration/time curve in the brain for POM-NS or POM-CMCS are reported. In line with the plasma levels, the administration of POM-NS led to higher brain concentrations as compared to POM-CMCS at each time point. After 0.5 h, the drug concentration in brain tissue for POM-NS was 0.90 μg/ml, a value three-fold higher than that of the coarse suspension (0.29 μg/ml). Furthermore, POM administered as a nanosuspension reached a peak brain level of 1.49 μg/ml after 2 h and, thereafter, was slowly and fully cleared by 48 h. In contrast, the coarse suspension generated a lower peak concentration (0.29 μg/ml), which rapidly decreased leading to full drug clearance after 24 h.

Notably, at 6 h following POM-NS administration brain drug levels were similar to concomitant plasma ones and were substantially greater than those in plasma at 24 h (Figure 8). This reflects a slower brain clearance with respect to the blood clearance for POM-NS, suggesting some accumulation of POM within brain tissue, in accord with its lipophilicity.

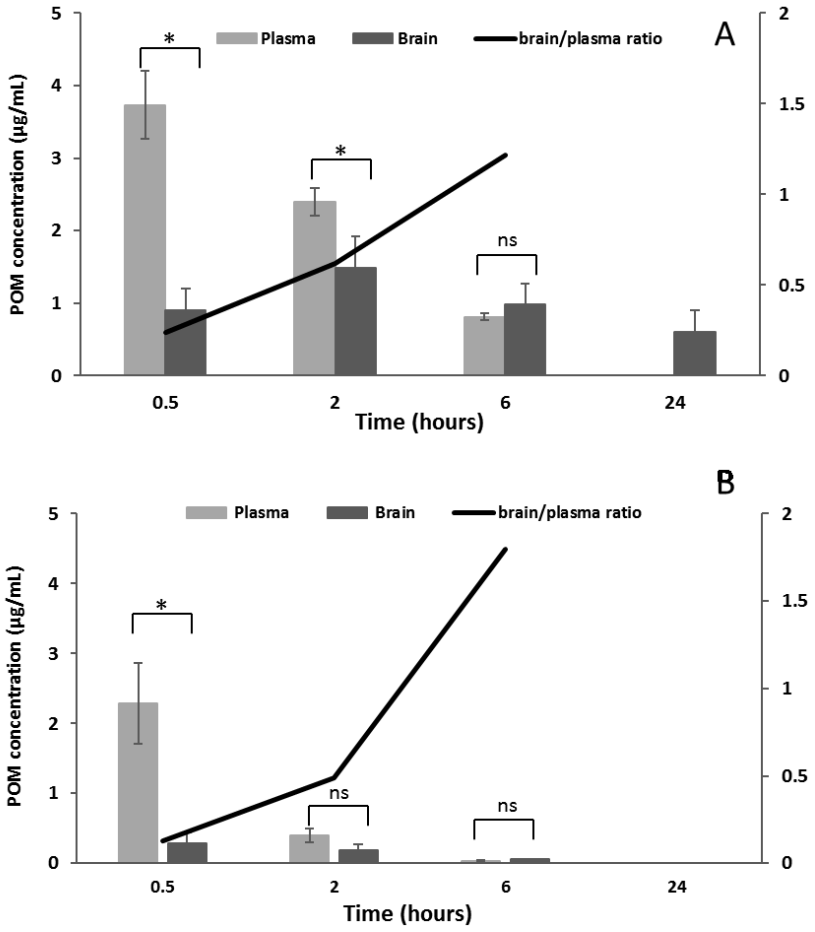

Figure 8. Plasma and brain POM concentration after i.p. administration of POM-NS (A) and POM-CMCS (B) at increasing time points (0.5, 2, 6, 24 h) and corresponding POM brain /plasma ratio. The asterisks indicate statistically significant data (* = $p < 0.05$), ns indicates no significant difference ($p > 0.05$).

4. Conclusions

The present study proposes the nanosizing process of the immunomodulatory imide drug Pomalidomide as an efficient strategy to improve the drug water solubility and consequently the bioavailability after an intraperitoneal administration. POM nanocrystals ensured increased plasma and brain levels when compared with POM coarse suspension. Specifically, both the higher and longer-lasting drug levels measured into the brain when POM is formulated as a nanosuspension are pivotal features that, together with the favorable toxicological aspects, position this drug among first choice compounds in the IMiDs class for repositioning in neurological disorders.

Funding: "This research was funded in part by: (i) the Intramural Research Program at the University of Cagliari (Università degli Studi di Cagliari), Italy, (ii) the Intramural Research Program of the National Institute on Aging, National Institutes of Health, Baltimore, MD, United States and (iii) UniCA- Progetti biennali d'Ateneo Finanziati dalla Fondazione di Sardegna- annualità 2018 CUPF74I19000950007.

Institutional Review Board Statement: All experimental procedures complied with the ARRIVE guidelines and were in accordance with the guidelines and protocols approved by the European Community (2010/63UE L 276 20/10/2010). Experimental protocols were approved by the Ministry of Health, Autorization n° 766/2020-PR (D.lgs. 26/2014).

Conflicts of Interest: The authors declare no conflict of interest.

References

Amidon, G.L., Lennernäs, H., Shah, V.P., Crison, J.R., 1995. A theoretical basis for a biopharmaceutic drug classification: the correlation of in vitro drug product dissolution and in vivo bioavailability. Pharm. Res. 12, 413–20.

Beurel, E., Toups, M., Nemeroff, C.B., 2020. The Bidirectional Relationship of Depression and Inflammation: Double Trouble. Neuron 107, 234–256. doi:10.1016/j.neuron.2020.06.002

Bristol Myers Squibb, 2020. U.S. Food and Drug Administration Approves Bristol Myers Squibb's Pomalyst® (pomalidomide) for AIDS-Related and HIV-Negative Kaposi Sarcoma.

Casu, M.A., Mocci, I., Isola, R., Pisanu, A., Boi, L., Mulas, G., Greig, N.H., Setzu, M.D., Carta, A.R., 2020. Neuroprotection by the Immunomodulatory Drug Pomalidomide in the Drosophila LRRK2WD40 Genetic Model of Parkinson's Disease. Front. Aging Neurosci. 12. doi:10.3389/fnagi.2020.00031

Chanan-Khan, A.A., Swaika, A., Paulus, A., Kumar, S.K., Mikhael, J.R., Rajkumar, S. V, Dispenzieri, A., Lacy, M.Q., 2013. Pomalidomide: the new immunomodulatory agent for the treatment of multiple myeloma. Blood Cancer J. 3, e143. doi:10.1038/bcj.2013.38

Corrias, F., Schlich, M., Sinico, C., Pireddu, R., Valenti, D., Fadda, A.M., Marceddu, S., Lai, F., 2017. Nile red nanosuspensions as investigative model to study the follicular targeting of drug nanocrystals. Int. J. Pharm. 524, 1–8. doi:10.1016/j.ijpharm.2017.03.042

Dues, D.J., Moore, D.J., 2020. LRRK2 and Protein Aggregation in Parkinson's Disease: Insights From Animal Models. Front. Neurosci. 14. doi:10.3389/fnins.2020.00719

Gao, L., Liu, G., Ma, J., Wang, X., Zhou, L., Li, X., Wang, F., 2013. Application of Drug Nanocrystal Technologies on Oral Drug Delivery of Poorly Soluble Drugs. Pharm. Res. 30, 307–324. doi:10.1007/s11095-012-0889-z

Ghadi, R., Dand, N., 2017. BCS class IV drugs: Highly notorious candidates for formulation development. J. Control. Release 248, 71–95. doi:10.1016/j.jconrel.2017.01.014

Hoffmann, M., Kasserra, C., Reyes, J., Schafer, P., Kosek, J., Capone, L., Parton, A., Kim-Kang, H., Surapaneni, S., Kumar, G., 2013. Absorption, metabolism and excretion of [14C]pomalidomide in humans following oral administration. Cancer Chemother. Pharmacol. 71, 489–501. doi:10.1007/s00280-012-2040-6

Jiang, Y., Wang, J., Rozewski, D.M., Kolli, S., Wu, C.-H., Chen, C.-S., Yang, X., Hofmeister, C.C., Byrd, J.C., Johnson, A.J., Phelps, M.A., 2014. Sensitive liquid chromatography/mass spectrometry methods for quantification of pomalidomide in mouse plasma and brain tissue. J. Pharm. Biomed. Anal. 88, 262–268. doi:10.1016/j.jpba.2013.08.036

Jung, Y.J., Tweedie, D., Scerba, M.T., Greig, N.H., 2019. Neuroinflammation as a Factor of Neurodegenerative Disease: Thalidomide Analogs as Treatments. Front. Cell Dev. Biol. 7, 1–24. doi:10.3389/fcell.2019.00313

Jung, Y.J., Tweedie, D., Scerba, M.T., Kim, D.S., Palmas, M.F., Pisanu, A., Carta, A.R., Greig, N.H., 2021. Repurposing Immunomodulatory Imide Drugs (IMiDs) in Neuropsychiatric and Neurodegenerative Disorders. Front. Neurosci. 15, 656921. doi:10.3389/fnins.2021.656921

Kuter, K.Z., Cenci, M.A., Carta, A.R., 2020. The role of glia in Parkinson's disease: Emerging concepts and therapeutic applications. Prog. Brain Res. 252, 131–168. doi:10.1016/bs.pbr.2020.02.004

Lai, F., Schlich, M., Pireddu, R., Fadda, A.M., Sinico, C., 2018. Nanocrystals as Effective Delivery Systems of Poorly Water-soluble Natural Molecules. Curr. Med. Chem. doi:10.2174/0929867326666181213095809

Lukas, G., Brindle, S.D., Greengard, P., 1971. The route of absorption of intraperitoneally administered compounds. J. Pharmacol. Exp. Ther. 178, 562–564.

Mahony, C., Erskine, L., Niven, J., Greig, N.H., Figg, W.D., Vargesson, N., 2013. Pomalidomide is nonteratogenic in chicken and zebrafish embryos and nonneurotoxic in vitro. Proc. Natl. Acad. Sci. U. S. A. 110, 12703–12708. doi:10.1073/pnas.1307684110

Manca, M.L., Lai, F., Pireddu, R., Valenti, D., Schlich, M., Pini, E., Ailuno, G., Fadda, A.M., Sinico, C., 2020. Impact of nanosizing on dermal delivery and antioxidant activity of quercetin nanocrystals. J. Drug Deliv. Sci. Technol. 55, 101482. doi:10.1016/J.JDDST.2019.101482

Moreira, A.L., 1993. Thalidomide exerts its inhibitory action on tumor necrosis factor alpha by enhancing mRNA degradation, Journal of Experimental Medicine. doi:10.1084/jem.177.6.1675

Müller, R.., Jacobs, C., Kayser, O., 2001. Nanosuspensions as particulate drug formulations in therapy. Adv. Drug Deliv. Rev. 47, 3–19.

Müller, R.H., Peters, K., 1998. Nanosuspensions for the formulation of poorly soluble drugs. I. Preparation by a size-reduction technique. Int. J. Pharm. 160, 229–237. doi:10.1016/S0378-5173(97)00311-6

554 Pramod, K., Suneesh, C.V., Shanavas, S., Ansari, S.H., Ali, J., 2015. Unveiling the compatibility of eugenol with formulation
555 excipients by systematic drug-excipient compatibility studies. J. Anal. Sci. Technol. 6, 34. doi:10.1186/s40543-015-0073-2

556 Sampaio, E.P., Sarno, E.N., Galilly, R., Cohn, Z.A., Kaplan, G., 1991. Thalidomide selectively inhibits tumor necrosis factor
557 alpha production by stimulated human monocytes. J. Exp. Med. 173, 699–703. doi:10.1084/jem.173.3.699

558 Siegel, D.S., Schiller, G.J., Song, K.W., Agajanian, R., Stockerl-Goldstein, K., Kaya, H., Sebag, M., Samaras, C., Malek, E.,
559 Talamo, G., Seet, C.S., Mouro, J., Pierceall, W.E., Zafar, F., Chung, W., Srinivasan, S., Agarwal, A., Bahlis, N.J., 2020.
560 Pomalidomide plus low-dose dexamethasone in relapsed refractory multiple myeloma after lenalidomide treatment failure.
561 Br. J. Haematol. 188, 501–510. doi:10.1111/bjh.16213

562 Szabó, Z.-I., Orbán, G., Borbás, E., Csicsák, D., Kádár, S., Fiser, B., Dobó, M., Horváth, P., Kiss, E., Budai, L., Dobos, J.,
563 Pálla, T., Őrfi, L., Völgyi, G., Tóth, G., 2021. Inclusion complexation of the anticancer drug pomalidomide with cyclodextrins:
564 fast dissolution and improved solubility. Heliyon 7, e07581. doi:10.1016/J.HELIYON.2021.E07581

565 Terpos, E., Kanellias, N., Christoulas, D., Kastritis, E., Dimopoulos, M.A., 2013. Pomalidomide: a novel drug to treat relapsed
566 and refractory multiple myeloma. Onco. Targets. Ther. 6, 531–538. doi:10.2147/OTT.S34498

567 Tsai, Y.-R., Tweedie, D., Navas-Enamorado, I., Scerba, M.T., Chang, C.-F., Lai, J.-H., Wu, J.C.-C., Chen, Y.-H., Kang, S.-J.,
568 Hoffer, B.J., de Cabo, R., Greig, N.H., Chiang, Y.-H., Chen, K.-Y., 2019. Pomalidomide Reduces Ischemic Brain Injury in
569 Rodents. Cell Transplant. 28, 096368971985007. doi:10.1177/0963689719850078

570 Tsai, Y.R., Chang, C.F., Lai, J.H., Wu, J.C.C., Chen, Y.H., Kang, S.J., Hoffer, B.J., Tweedie, D., Luo, W., Greig, N.H., Chiang,
571 Y.H., Chen, K.Y., 2018. Pomalidomide ameliorates H2O2-induced oxidative stress injury and cell death in rat primary cortical
572 neuronal cultures by inducing anti-oxidative and anti-apoptosis effects. Int. J. Mol. Sci. 19, 3252. doi:10.3390/ijms19103252

573 Tweedie, D., Frankola, K.A., Luo, W., Li, Y., Greig, N.H., 2011. Thalidomide Analogues Suppress Lipopolysaccharide-
574 Induced Synthesis of TNF-α and Nitrite, an Intermediate of Nitric Oxide, in a Cellular Model of Inflammation. Open
575 Biochem. J. 5, 37–44. doi:10.2174/1874091X01105010037

576 Vargesson, N., Mahony, C., Erskine, L., Niven, J., Greig, N.H., Figg, W.D., 2013. Reply to D'Amato et al. and Zeldis et al.:
577 Screening of thalidomide derivatives in chicken and zebrafish embryos. Proc. Natl. Acad. Sci. U. S. A.
578 doi:10.1073/pnas.1318475110

579 Wager, T.T., Hou, X., Verhoest, P.R., Villalobos, A., 2010. Moving beyond Rules: The Development of a Central Nervous
580 System Multiparameter Optimization (CNS MPO) Approach To Enable Alignment of Druglike Properties. ACS Chem.
581 Neurosci 1, 435–449. doi:10.1021/cn100008c

582 Wang, Jing Ya, Huang, Y.N., Chiu, C.C., Tweedie, D., Luo, W., Pick, C.G., Chou, S.Y., Luo, Y., Hoffer, B.J., Greig, N.H.,
583 Wang, Jia Yi, 2016. Pomalidomide mitigates neuronal loss, neuroinflammation, and behavioral impairments induced by
584 traumatic brain injury in rat. J. Neuroinflammation 13. doi:10.1186/s12974-016-0668-6

585 Wang, Y., Tan, X., Fan, X., Zhao, L., Wang, S., He, H., Yin, T., Zhang, Y., Tang, X., Jian, L., Jin, J., Gou, J., 2021. Current
586 strategies for oral delivery of BCS IV drug nanocrystals: challenges, solutions and future trends. Expert Opin. Drug Deliv.
587 18, 1211–1228. doi:10.1080/17425247.2021.1903428

588